High Level Kinematic and Low Level Nonlinear Dynamic Control of Unmanned Ground Vehicles

Béla Lantos, Zsófia Bodó

Budapest University of Technology and Economics, Hungary
H-1117 Budapest, Magyar Tudósok krt. 2., Hungary
E-mail: *lantos@iit.bme.hu*, *zsbodo@iit.bme.hu*

Abstract: High level kinematic model-based control of vehicles is an often used technique in the presence of a driver. Existing robust low level linear (speed, steering, brake, suspension etc.) control components are available in cars which can be influenced using the outputs of the kinematic control as reference signals. If problems arise then the driver can modify the internal control based on the visual information of the path and the observed car motion. In case of unmanned ground vehicles (UGVs) this modification is no more evident. In the paper an approach is presented to estimate the errors in real UGV situations where the road-tire contacts generate special sliding effects in behavior of the UGV. These effects are considered as disturbances and are involved in both the kinematic and dynamic models. The novelties of the paper are the consideration of the sliding effects in the kinematic control and the application of sophisticated nonlinear methods for low level dynamic control. It is demonstrated by simulation that high level kinematic control based approaches can cause lateral errors in the order of 1m. In the experiments three types of low level dynamic controls were considered: i) a simplified one using the steering angle of kinematic control, ii) nonlinear input-output linearization (DGA method), and iii) flatness control. They can supply the sliding angle information for the kinematic control.

Keywords: Kinematic Control, Sliding Effects, UGV, Kinematic and Dynamic Coupling, Path Following, Input-Output Linearization, Flatness Control

1 Introduction

Vehicle control based on the kinematic model is a popular approach delivering speed and steering angle commands for the existing robust low level control subsystems. If problems arise and a driver is present then the necessary corrections can be performed manually using the available visual information and the observed difference between the path and the car's motion. However, in case of unmanned ground vehicles (UGVs) this modification is no more possible.

In the paper an approach is presented to estimate the errors in real UGV situations where the road-tire contacts generate special sliding effects in the dynamic behavior of the UGV. These effects are usually not considered in the kinematic modeling where the side motion of the vehicle is neglected and nonholonomic constraints are assumed for the front and rear wheels, see e.g. De Luca and coworkers [1].

A remarkable exception is the approach of Arogeti and Berman [2] whose method can also manage the sliding effects involved in the kinematic model in the form of disturbances. Their method is based on the results of Scherer and Weiland [3] for decreasing the peak-to-peak L_∞ (or generalized H_2) disturbance effects in single variable (SISO) systems. Arogeti and Berman involved the sliding effects in the kinematic model and presented a modified path following kinematic control method. Since the kinematic and dynamic models are coupled through the sliding effects therefore a realistic testing cannot be performed without an appropriate dynamic control method. The paper [2] demonstrates using simulation that with the modified kinematic control the slip angles remain in realistic and acceptable domains. Unfortunately, it cannot be pointed out from [2] what was the dynamic control method during the test. Similarly, no data was shown about the path following errors.

Our earlier paper [4] considered the similar problem but the main goal was to show what is the order of the lateral error if the steering angle of the modified kinematic control is saved in the low level dynamic control, and if it is large, how can it be decreased by dynamic control. Since kinematic and dynamic models are coupled through the slip angles hence realistic dynamic control of the velocity and the acceleration is needed for correct analysis of the lateral error (the slip angles depend on the velocities and the steering angle). For this purpose a dynamic control was also developed which is based on nonlinear input-output linearization (dynamic inversion). The main novelty of our present paper is the extension of the dynamic control methods with the nonlinear flatness control and the proof of the flatness property both for front and rear wheel driven cars.

Other popular methods exist using PID-type control of linekeeping [5], potential field technique [6] and nonlinear time-optimal control [7].

The paper is organized as follows. Section 2 presents the modified kinematic control if the slip angles are taken into consideration and the disturbance effects have to be reduced. Section 3 deals with the suggested nonlinear dynamic control methods for testing. Section 4 shows the numerical results of the simulation for the parallel running modified kinematic and dynamical control and the analysis of the lateral error. Section 5 concludes the paper.

2 MODIFIED KINEMATIC CONTROL

For the kinematic and dynamical investigations in the paper the well known two wheel bicycle model will be used, see Fig. 1. The notations are as usual, i.e. front (F) and rear (R) are wheels, longitudinal (l), and transversal (t) stand for forces, M is the moment, CoG is the center of gravity, v is velocity, β stands for the side slip

angle, α denote the slip angles of the wheels, ψ is the orientation (heading), and δ_w is the steering angle in the figure. The other parameters are geometrical ones and $L := l_R + l_F$. From the frames x_0 and y_0 is the inertia system, x_{CoG} and y_{CoG} is the body system and x_w and y_w is the front wheel system. In the paper front wheel steering and rear wheel accelerating are assumed.

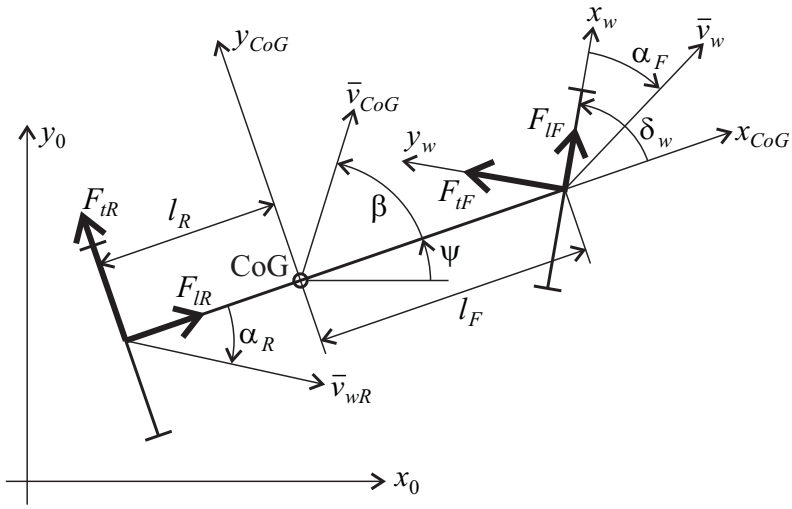

Figure 1
The two wheel (bicycle) structure

For path design and kinematic modeling the coordinate system will be fixed to the middle point of the rear axle instead of the CoG. Kinematic models satisfying the nonholonomic constraints can be brought to chain form and stabilized by state feedback [1].

The convergence of error decaying strongly depends on the speed variable $\bar{v} = \dot{x} = \cos(\psi)v$ that depends also on the orientation ψ. Furthermore, the singularities of the chain transformation should be avoided during path design.

The modified form will be discussed in two steps. First the error definition is modified and after it the slip angles will be taken into consideration.

2.1 Modified error definition for the chain form

In order to eliminate the dependence of the control u on the orientation, the basic paper of Arogeti and Berman [2] defines the tracking error by

$$\begin{aligned} e_1 &= f(x) - y \\ e_2 &= f'(x)\cos(\psi) - \sin(\psi) \\ e_3 &= f''(x)\cos^2(\psi) - \frac{\tan(\delta_w)}{L}\left(f'(x)\sin(\psi) + \cos(\psi)\right) \end{aligned} \tag{1}$$

where e_1 represents the position error in lateral direction, e_2 is the orientation error and e_3 is the steering error, and $y_d = f(x)$ is the desired path.

Denote v the absolute value (magnitude) of the velocity in the middle point of the rear axle (i.e. $\bar{v} := v$) which makes a great difference to the original method because v does not depend on the orientation ψ.

The transformation to the chain form is completed by the control signal

$$\begin{aligned} w = &\Big[\Big(f'''(x)\cos^3(\psi) - 3\frac{f''(x)\cos(\psi)\sin(\psi)\tan(\delta_w)}{L} \\ &- \frac{f'(x)\cos(\psi)\tan^2(\delta_w)}{L^2} + \frac{\sin(\psi)\tan^2(\delta_w)}{L^2}\Big)v - u\Big] \\ &\times \frac{L\cos^2(\delta_w)}{f'(x)\sin(\psi) + \cos(\psi)} \end{aligned} \tag{2}$$

where u is the stabilizing state feedback.

The new chain form is

$$\dot{e}_1 = e_2 v, \quad \dot{e}_2 = e_3 v, \quad \dot{e}_3 = u \tag{3}$$

The physical interpretation of e_1 is the vehicle lateral error and e_2 is the orientation (heading) error. Along the path e_1 and e_2 are zero hence the reference value of the orientation is $\tan(\psi_r(x)) = f'(x)$, i.e.

$$\psi_r(x) = \arctan(f'(x)) \tag{4}$$

Considering e_3 for $e_2 = 0$ it yields $f'(x)\sin(\psi_r) + \cos(\psi_r) = \tan(\psi_r)\sin(\psi_r) + \cos(\psi_r) = 1/\cos(\psi_r)$ and one obtains for $e_3 = 0$:

$$\tan(\delta_{wr}) = Lf''(x)\cos^3(\psi_r) \tag{5}$$

2.2 Kinematic control in the presence of sliding effects

The earlier discussion assumed rolling without side motion (slipping) of the wheels. Considering the bicycle model, the velocity vector v_R, the slip angles α_R and α_F and denoting the projection of the velocity vector in x-direction of the car by $v = |v_R|\cos(\alpha_R) \Leftrightarrow |v_R| = v/\cos(\alpha_R)$, then the kinematic equations in the presence of sliding effects can be written as follows:

$$\begin{aligned} \dot{x} &= \frac{\cos(\psi + \alpha_R)}{\cos(\alpha_R)} v = (\cos(\psi) - \tan(\alpha_R)\sin(\psi))\, v \\ \dot{y} &= \frac{\sin(\psi + \alpha_R)}{\cos(\alpha_R)} v = (\sin(\psi) - \tan(\alpha_R)\cos(\psi))\, v \\ \dot{\psi} &= \frac{\tan(\delta_w - \alpha_F) + \tan(\alpha_R)}{L} v \\ \dot{\delta}_w &= w \end{aligned} \tag{6}$$

The design objective is to follow the prescribed reference path $y_d = f(x)$. Using (1), (2) and (6) the tracking error can be written in the form consisting of two components:

$$\begin{bmatrix} \dot{e}_1 \\ \dot{e}_2 \\ \dot{e}_3 \end{bmatrix} = \begin{bmatrix} e_2 v \\ e_3 v \\ u \end{bmatrix} + \begin{bmatrix} g_1(\psi, f', \alpha_R) \\ g_2(\psi, \delta_w, f', f'', \alpha_R, \alpha_F) \\ g_3(\psi, \delta_w, f', f'', f''', \alpha_R, \alpha_F) \end{bmatrix} v \tag{7}$$

The functions g_1, g_2 and g_3 are nonlinear functions defined in [2]. The vehicle heading ψ_r and steering angle δ_{wr} along the path are given in (4) and (5). This second nonlinear term in (7) can be linearized in a small neighborhood of the desired path and the zero slip angles resulting in

$$\begin{aligned} \dot{e} = & \underbrace{\begin{bmatrix} 0 & 1 & 0 \\ 0 & 0 & 1 \\ 0 & 0 & 0 \end{bmatrix}}_{A} v e + \underbrace{\begin{bmatrix} 0 \\ 0 \\ 1 \end{bmatrix}}_{B_2} u \\ & + \underbrace{\begin{bmatrix} \bar{g}_{11}(\psi_r) & 0 \\ \bar{g}_{21}(\psi_r, \delta_{wr}) & \bar{g}_{22}(\psi_r, \delta_{wr}) \\ \bar{g}_{31}(\psi_r, \delta_{wr}, f''') & \bar{g}_{32}(\psi_r, \delta_{wr}) \end{bmatrix}}_{B_1(t)=B_1(\psi_r, \delta_{wr}, f''')} v \underbrace{\begin{bmatrix} \alpha_R \\ \alpha_F \end{bmatrix}}_{d(t)} \end{aligned} \tag{8}$$

2.3 Robust kinematic control

For an LTI systems of class $\dot{e} = Ae + Bd$, $z = Ce$, $e \in R^n$, $d \in R^m$ and $z \in R^p$ Scherer and Weiland [3] developed a method for the design of a control u satisfying peak–to–peak performance, i.e. $||z||_\infty \leq \gamma ||d||_\infty$ for given $\gamma > 0$ based on LMI technique.

The functions g_i and $\bar{g}_{ij}$ are listed in Arogeti and Berman [2] without derivation. Because of the central role of these functions their validity was also checked by the authors of this paper. In the sequel some detected errors of the above paper are also corrected, especially the correct order of the terms to find upper bounds for $B_1(t)B_1^T(t) < \bar{B}_1\bar{B}_1^T$, $\forall t$.

The model (8) consists of two parts. The first part is the new chain form $\dot{e} = Aev + B_2 u$ according to (3), while the second $B_1(\psi_r, \delta_{wr}, f''')vd(t)$ can be treated as an unknown model disturbance. The matrix $B_1(\cdot)$ is a function of the reference path thus all its elements are bounded, i.e. they are in L_∞, thus the robust design approach should be based on the nonstandard L_∞ valued performance optimization. Notice that model (8) belongs to the LTI system class in [2] with $n = 3$ and $m = 2$.

First we considered the 3×3 type matrix $B_1(t)B_1(t)^T$ along the path and determined a constant matrix $\bar{B}_1$ satisfying $B_1(t)B_1^T(t) < \bar{B}_1\bar{B}_1^T$ for $\forall t$.

Notice that model (8) belongs to the LTI system class in [2] with $n = 3$, $m = 2$ and $p = 4$. Consider for $e(0) = 0$ the linear time-varying system

$$\begin{aligned} \dot{e}(t) &= Av(t)e(t) + B_2 u(t) + B_1 v(t) d(t) \\ z(t) &= Ce(t) + Du(t) \end{aligned} \tag{9}$$

with the input $u \in R$, $d \in R^2$ and the controlled output $z \in R^p$ and the bounds

$$\begin{aligned} 0 < \eta_1 < v(t) < \eta_2 < \infty \\ B_1(t)B_1^T(t) < \bar{B}_1\bar{B}_1^T \end{aligned} \tag{10}$$

Using the state feedback $u(t) = Ke(t)v(t)$ the closed loop system will be

$$\begin{aligned} \dot{e}(t) &= (A + B_2K)v(t)e(t) + B_2u(t) + B_1v(t)d(t) \\ z(t) &= (C + DKv(t))e(t) = \bar{C}e(t) \end{aligned} \tag{11}$$

Based on the results of [3] and using the bounds in (10) it was shown in [2] that given the system (11) and a scalar $\gamma > 0$, assume there exist $0 < \lambda \in R$, $0 < Q \in R^{n\times n}$ and $Y \in R^{p\times n}$ such that the two LMIs are satisfied, i.e.

$$\begin{aligned} &\begin{bmatrix} (QA^T + AQ + Y^TB_2^T + B_2Y)\eta_1 + \lambda nQ & \bar{B}_1\eta_2 \\ \bar{B}_1^T\eta_2 & -\gamma I_m \end{bmatrix} < 0 \\ &\begin{bmatrix} \lambda Q & QC^T + Y^TD^T \\ CQ + DY & \gamma I_p \end{bmatrix} > 0 \end{aligned} \tag{12}$$

Then, for control gains given by $K = YQ^{-1}$, the closed loop system norm satisfies $||L_{cl}||_\infty < \gamma$, and the system is internally asymptotically stable. Notice yet that the two LMIs are coupled in Q and Y that determine the state feedback K.

3 ADVANCED NONLINEAR DYNAMIC CONTROL

The dynamic model of the vehicle will be considered in the frame fixed to CoG while the origin of the frame used for kinematic control is at the middle point of the rear axle. Fortunately, the two frames are parallel. For simplicity denote v_G the absolute value of the velocity at CoG. The angles β, α_F, α_R are usually called the vehicle body side slip angle, the tire slide slip angle front and the tire slide slip angle rear, respectively.

The tire slip angles are defined by

$$\tan(\alpha_R) = \frac{l_R\dot{\psi} - v_G\sin(\beta)}{v_G\cos(\beta)} \tag{13}$$

$$\tan(\delta_W - \alpha_F) = \frac{l_F\dot{\psi} + v_G\sin(\beta)}{v_G\cos(\beta)} \tag{14}$$

The forces acting at the origin of the coordinate system of the front wheel are the longitudinal force F_{lF} and the transversal force F_{tF}. It should be underlined that in the state equations of the *dynamic modeling* the transversal forces are described by the Pacejka's equations [8] in order to obtain reliable results for the lateral errors. On the other hand, during the *dynamic control design*, as usual in the vehicle control literature, the lateral forces are approximated by the cornering stiffnesses, in order to omit nonlinear dynamic optimization in real time.

3.1 Input affine dynamic model for control design

For dynamic control design it is assumed that the transversal components are $F_{tF} = c_F \alpha_F$ and $F_{tR} = c_R \alpha_R$, respectively, where the cornering stiffnesses c_F and c_R are constants. Assuming small $\delta_W - \alpha_F$, α_R and β and using the approximations $\tan(\delta_W - \alpha_F) \approx \delta_W - \alpha_F$, $\tan(\alpha_R) \approx \alpha_R$, $\sin(\beta) \approx \beta$ and $\cos(\beta) \approx 1$ it follows

$$\alpha_F = \delta_W - \beta - \frac{l_F \dot{\psi}}{v_G}, \quad \alpha_R = -\beta + \frac{l_R \dot{\psi}}{v_G}$$

Applying the usual notations $\cos(\beta) = C_\beta$, $\sin(\beta) = S_\beta$, and the differentiation rule in moving frames, then the kinematic model and based on it the dynamic model of the car can be derived.

$$\begin{aligned} \bar{v}_{COG} &= \begin{pmatrix} C_\beta & S_\beta & 0 \end{pmatrix}^T v_G \\ \bar{a}_{COG} &= \dot{\bar{v}}_{COG} + \omega \times \bar{v}_{COG} \\ &= \begin{bmatrix} C_\beta & -v_G S_\beta \\ S_\beta & v_G C_\beta \\ 0 & 0 \end{bmatrix} \begin{pmatrix} \dot{v}_G \\ \dot{\beta} \end{pmatrix} + \begin{pmatrix} -S_\beta \\ C_\beta \\ 0 \end{pmatrix} \dot{\psi} v_G \end{aligned}$$

Taking into account the direction of the forces, dividing by the mass m_v of the car, and considering only the nontrivial components of $\bar{a}_{COG}$, the acceleration is obtained:

$$\bar{a}_{COG} = \frac{1}{m_v} \begin{pmatrix} F_x \\ F_y \end{pmatrix} = \frac{1}{m_v} \begin{pmatrix} F_{lF} C_{\delta_w} - F_{tF} S_{\delta_w} + F_{lR} \\ F_{lF} S_{\delta_w} + F_{tF} C_{\delta_w} + F_{tR} \end{pmatrix}$$

3.2 Nominal dynamic control saving kinematic steering angle

Because forward axle steering and rear axle driving are assumed in this paper therefor the (e.g. industrial) low level dynamic control can be modeled in such a simple form that the rear longitudinal force is determined from the state equation and the steering angle of the kinematic control is used as steering angle of the dynamic control. This approach will be called *nominal control*. The driving force in nominal control can easily be computed:

$$F_{lR} = m_v(\dot{v}_{cx} - v_{cy}\dot{\psi}) + F_{tF} S_{\delta_w} \tag{15}$$

The differentiation of v_{cx} can be approximated by a fictitious control loop, see also [5], but with other choice of the parameters in the fictitious controller.

3.3 Differential Geometry Based Control Algorithm

It is useful to introduce the rear ($S_h = F_{tR}$) and front ($S_v = F_{tF}$) side forces where

$$S_h = c_R(-\beta + l_R \dot{\psi}/v_G), \tag{16}$$

$$S_v = c_F(\delta_w - \beta - l_F \dot{\psi}/v_G). \tag{17}$$

It is clear that steering angle δ_w can be determined for control implementation by

$$\delta_w = \frac{1}{c_F} S_v + \beta + l_F \dot{\psi} / v_G \tag{18}$$

Assuming small angles the input affine model arises as

$$\dot{x} = \begin{bmatrix} -x_3 + S_h/(m_v x_4) \\ x_3 \\ -S_h l_R / I_z \\ 0 \\ x_4 C_{12} \\ x_4 S_{12} \end{bmatrix} + \begin{bmatrix} 1/(m_v x_4) & -x_1/(m_v x_4) \\ 0 & 0 \\ l_F/I_z & 0 \\ 0 & 1/m_v \\ 0 & 0 \\ 0 & 0 \end{bmatrix} u, \tag{19}$$

$$\dot{x} = A(x) + B(x)u, \quad y = (x_5, x_6)^T = C(x),$$
$$x = (\beta, \psi, \dot{\psi}, v_G, X, Y)^T, \; u = (S_v, F_{lR})^T, \; y = (X, Y)^T.$$

Here we used the notation $C_{12} = \cos(x_1 + x_2)$ etc. and X and Y are the coordinates of the CoG in the inertia frame.

It can be shown [9] that the above approximated dynamic model has vector relative degrees $r_1 = r_2 = 2$. Thus (the observable subsystem) has the form

$$\begin{pmatrix} \ddot{y}_1 \\ \ddot{y}_2 \end{pmatrix} = q(x) + S(x)u \tag{20}$$

$$S(x) = \frac{1}{m_v} \begin{bmatrix} -S_{12} & C_{12} + x_1 S_{12} \\ C_{12} & S_{12} - x_1 C_{12} \end{bmatrix}, \tag{21}$$

$$q(x) = \frac{1}{m_v} \begin{pmatrix} -S_{12} \\ C_{12} \end{pmatrix} S_h. \tag{22}$$

Hence the system can be input-output linearized by an internal nonlinear feedback and the resulting system consists of two double integrators:

$$u := S^{-1}[v - q(x)], \tag{23}$$
$$\ddot{y}_i = v_i, \;\; i = 1, 2 \tag{24}$$

The stability of the zero dynamics was proven in [9].

First we assume a prescribed stable and sufficiently quick error dynamics

$$(\ddot{y}_{di} - \ddot{y}_i) + \alpha_{1i}(\dot{y}_{di} - \dot{y}_i) + \lambda_i(y_{di} - y_i) = 0 \tag{25}$$

Let us use the notation $w_i := y_{di} + (\alpha_{1i}\dot{y}_{di} + \ddot{y}_{di})/\lambda_i$, then

$$\ddot{y}_i = v_i = \lambda_i w_i - \alpha_{1i}\dot{y}_i - \lambda_i y_i \tag{26}$$

Observe that $\lambda_i w_i$ depends only on the reference signal and its derivatives (feed forward from the reference signal) and $-\alpha_{1i}\dot{y}_i - \lambda_i y_i$ is the state feedback stabilizing

the system where α_{1i} and λ_i are positive for stable error dynamics. Let $\lambda_1 = \lambda_2 := \lambda$, $\alpha_{11} = \alpha_{12} = 2\sqrt{\lambda}$ (or similar ones) where $\lambda > 0$, then two decoupled linear systems are arising whose characteristic equation and differential equation are, respectively,

$$s^2 + 2\sqrt{\lambda}s + \lambda = 0 \Rightarrow s_{1,2} = -\sqrt{\lambda}, \tag{27}$$

$$\ddot{y}_i + \alpha_{1i}\dot{y}_i + \lambda y_i = \lambda_i w_i. \tag{28}$$

The steps of the *DGA Control Algorithm (DGA)*:

1. $w_i := y_{di} + \frac{1}{\lambda_i}(\alpha_{1i}\dot{y}_{di} + \ddot{y}_{di}),\ \ i = 1,2$
2. $\bar{y}_1 := \lambda_1 w_1 - \alpha_{11}(x_4 C_{12}) - \lambda_1 x_5$
3. $\bar{y}_2 := \lambda_2 w_2 - \alpha_{12}(x_4 S_{12}) - \lambda_2 x_6$
4. $S_h := c_R\,[-x_1 + (l_R x_3 / x_4)]$
5. $u_1 := -S_h + m_v\,[(x_1 C_{12} - S_{12})\bar{y}_1 + (x_1 S_{12} + C_{12})\bar{y}_2]$
6. $u_2 := m_v(C_{12}\bar{y}_1 + S_{12}\bar{y}_2)$
7. $\delta_w := (u_1 / c_F) + x_1 + (l_F x_3 / x_4)$
8. $F_{lR} := u_2$

Notice, because not all state variables can be measured, a state estimator has to be implemented in order to supply the necessary state information for the controller. This problem was discussed in Chapter 5, pp. 189-195 of [9].

3.4 Flatness control

A nonlinear system $\dot{x} = f(x,u)$, $x \in R^n$, $u \in R^m$ is said to be differentially flat if there exists a vector $y = (y_1, \ldots, y_m)^T \in R^m$ called the flat output and vector valued functions and integers such that $y = h(x, u, \dot{u}, \ldots, u^{(r)})$, $x = A(y, \dot{y}, \ldots, y^{(r_x)})$, and $u = B(y, \dot{y}, \ldots, y^{(r_u)})$, see [10] and [9]. Notice that y and u have equal dimension.

The two wheels (bicycle) vehicle dynamic model can be approximated by using the flat outputs $y_1 = V_x$ and $y_2 = l_F m V_y - I_z \dot{\psi}$, and the controls $u_1 = T_m - T_b$ and $u_2 = \delta_w$, respectively.

3.4.1 Flatness proof for front wheel or rear wheel driven cars

A sketch of the flatness proof can be found for front steering and front driving in the recent paper [11]. Since rear wheel driving is used in the kinematical part of our paper hence a generalization for both driving cases will be given.

In order to show the similarities and/or differences we will use a similar notation as the cited paper. Most of the notations are evident: for simplicity we omit the index w in δ_w; V_x and V_y are the velocity components of CoG; instead of l (longitudinal) and t (transversal) indexes of forces the indexes x and y will be used. It will be

assumed that the braking forces satisfy $T_{br} = rT_{bf}$, $r \in [0,1]$, hence the total braking force is $T_b = (1+r)T_{bf}$ and thus

$$T_{bf} = \frac{1}{1+r}T_b, \quad T_{br} = \frac{r}{1+r}T_b \tag{29}$$

Denote the tire effective radius R, the wheel inertia I_ω and the wheel angular velocities ω_f and ω_r, respectively. The wheel angular velocities are assumed to be measured by odometers.

For *front wheel driven car* yields:

$$\begin{aligned} F_{xf} &= \frac{1}{R}\left(-I_\omega \dot{\omega}_f + T_m - T_{bf}\right) \\ F_{xr} &= \frac{1}{R}\left(-I_\omega \dot{\omega}_r - T_{br}\right) \end{aligned} \tag{30}$$

For *rear wheel driven car* yields:

$$\begin{aligned} F_{xf} &= \frac{1}{R}\left(-I_\omega \dot{\omega}_f - T_{bf}\right) \\ F_{xr} &= \frac{1}{R}\left(-I_\omega \dot{\omega}_r + T_m - T_{br}\right) \end{aligned} \tag{31}$$

The basic dynamic motion equations are as follows:

$$\begin{aligned} m(\dot{V}_x - \dot{\psi}V_y) &= F_{xf}\cos(\delta) - F_{yf}\sin(\delta) + F_{xr} \\ m(\dot{V}_y + \dot{\psi}V_x) &= F_{xf}\sin(\delta) + F_{yf}\cos(\delta) + Fyr \\ I_z\ddot{\psi} &= l_F\left(F_{yf}\cos(\delta) + F_{xf}\sin(\delta)\right) - l_R F_{yr} \end{aligned} \tag{32}$$

Assuming as usual small angles and lateral forces approximated by using cornering stiffness the above equations can be simplified.

For front wheel driven car:

$$\begin{aligned} \dot{V}_x &= \dot{\psi}V_y - \frac{I_\omega}{mR}(\dot{\omega}_r + \dot{\omega}_f) + \frac{1}{mR}(T_m - T_b) + \frac{c_F}{m}\frac{V_y + l_F\dot{\psi}}{V_x}\delta - \frac{c_F}{m}\delta^2 \\ \dot{V}_y &= -\dot{\psi}V_x - \frac{c_F}{m}\frac{V_y + l_F\dot{\psi}}{V_x} - \frac{c_R}{m}\frac{V_y - l_R\dot{\psi}}{V_x} + \frac{1}{mR}(T_m - T_{bf})\delta + \frac{c_F R - I_\omega\dot{\omega}_f}{mR}\delta \\ \ddot{\psi} &= \frac{1}{I_z}\left[-l_F c_F\frac{V_y + l_F\dot{\psi}}{V_x} + l_R c_R\frac{V_y - l_R\dot{\psi}}{V_x} + \frac{l_F}{R}(T_m - T_{bf})\delta + \frac{l_F}{R}(c_F R - I_\omega\dot{\omega}_f)\delta\right] \end{aligned} \tag{33}$$

For rear wheel driven car:

$$\begin{aligned} \dot{V}_x &= \dot{\psi}V_y - \frac{I_\omega}{mR}(\dot{\omega}_r + \dot{\omega}_f) + \frac{1}{mR}(T_m - T_b) + \frac{c_F}{m}\frac{V_y + l_F\dot{\psi}}{V_x}\delta - \frac{c_F}{m}\delta^2 \\ \dot{V}_y &= -\dot{\psi}V_x - \frac{c_F}{m}\frac{V_y + l_F\dot{\psi}}{V_x} - \frac{c_R}{m}\frac{V_y - l_R\dot{\psi}}{V_x} - \frac{1}{mR}T_{bf}\delta + \frac{c_F R - I_\omega\dot{\omega}_f}{mR}\delta \\ \ddot{\psi} &= \frac{1}{I_z}\left[-l_F c_F\frac{V_y + l_F\dot{\psi}}{V_x} + l_R c_R\frac{V_y - l_R\dot{\psi}}{V_x} - \frac{l_F}{R}T_{bf}\delta + \frac{l_F}{R}(c_F R - I_\omega\dot{\omega}_f)\delta\right] \end{aligned} \tag{34}$$

As can be seen, the differences in the two driving modes are in $\dot{V}_y$ and $\ddot{\psi}$. Moreover, if $u_1 = T_m - T_b$ is already known then for $u_1 > 0 \Rightarrow T_m = u_1, T_b = 0$ while for $u_1 \leq 0 \Rightarrow T_m = 0, T_b = -u_1$ can be chosen and T_{bf}, T_{br} can also be computed using the selected value of r.

Hence the two driving modes can be standardized using the notation $\gamma(u_1) = T_m - T_b$ for rear wheel driven car and $\gamma(u_1) = -T_b$ for front wheel driven car, respectively.

With the notations

$$f(x) = \begin{bmatrix} \dot{\psi} V_y - \frac{I_\omega}{mR}(\dot{\omega}_r + \dot{\omega}_f) \\ -\dot{\psi} V_x - \frac{c_F}{m}\frac{V_y + l_F\dot{\psi}}{V_x} - \frac{c_R}{m}\frac{V_y - l_R\dot{\psi}}{V_x} \\ \frac{1}{I_z}\left(-l_F c_F \frac{V_y + l_F\dot{\psi}}{V_x} + l_R c_R \frac{V_y - l_R\dot{\psi}}{V_x}\right) \end{bmatrix}$$

$$g(x) = \begin{bmatrix} \frac{1}{mR} & \frac{c_F}{m}\frac{V_y + l_F\dot{\psi}}{V_x} \\ 0 & \frac{c_F R - I_\omega \dot{\omega}_f}{mR} \\ 0 & \frac{l_F}{I_z R}(c_F R - I_\omega \dot{\omega}_f) \end{bmatrix}, \quad g_1 = \begin{bmatrix} 0 \\ \frac{1}{mR} \\ \frac{l_R}{I_z R} \end{bmatrix}, \quad g_2 = \begin{bmatrix} -\frac{c_F}{m} \\ 0 \\ 0 \end{bmatrix} \tag{35}$$

the state equation can be written as follows:

$$\dot{x} = f(x) + g(x)u + g_1\gamma(u_1)u_2 + g_2 u_2^2 \tag{36}$$

It remains to prove the flatness of the system for the outputs $y_1 = V_x$ and $y_2 = l_F m V_y - I_z\dot{\psi}$. Using the earlier results and adding zero in special form yields

$$\begin{aligned} \dot{y}_2 =& l_F\left[-m\dot{\psi}V_x - c_F\frac{V_y + l_F\dot{\psi}}{V_x} - c_R\frac{V_y - l_R\dot{\psi}}{V_x} + \frac{1}{R}\gamma(u_1)\delta + \frac{c_F R - I_\omega\dot{\omega}_f}{R}\delta\right] \\ &+ \left[l_F c_F\frac{V_y + l_F\dot{\psi}}{V_x} - l_R c_R\frac{V_y - l_R\dot{\psi}}{V_x} - \frac{l_F}{R}\gamma(u_1)\delta - \frac{l_F}{R}(c_F R - I_\omega\dot{\omega}_f)\delta\right] \\ &+ (l_F c_R - l_F c_R)\frac{V_y - l_R\dot{\psi}}{V_x} \end{aligned}$$

Now we can cancel the appropriate positive and negative terms in pair and obtain

$$\dot{y}_2 = -l_F m\dot{\psi}V_x - (l_F + l_R)c_R\frac{V_y - l_R\dot{\psi}}{V_x} \tag{37}$$

Multiplying with $y_1 = V_x$ it follows

$$y_1\dot{y}_2 = \left[-l_F m y_1^2 + (l_F + l_R)c_R l_R\right]\dot{\psi} - (l_F + l_R)c_R\frac{y_2 + I_z\dot{\psi}}{l_F m}$$

from which $\dot{\psi}$ and V_y can be determined:

$$\dot{\psi} = -\frac{l_F m y_1\dot{y}_2 + (l_F + l_R)c_R y_2}{(l_F + l_R)c_R(I_z - l_F l_R m) + (l_F m y_1)^2} \tag{38}$$

$$V_y = \frac{y_2 + I_z\dot{\psi}}{l_F m} = \frac{y_2}{l_F m} - \frac{I_z}{l_F m}\frac{l_F m y_1\dot{y}_2 + (l_F + l_R)c_R y_2}{(l_F + l_R)c_R(I_z - l_F l_R m) + (l_F m y_1)^2} \tag{39}$$

Hence $x = (V_x, V_y, \dot{\psi})^T = A(y_1, y_2, \dot{y}_2)$ and $r_x = 1$.

Unfortunately, to the flatness property of u we need also $\ddot{y}_2$:

$$\ddot{y}_2 = -l_F m \ddot{\psi} V_x - l_F m \dot{\psi} \dot{V}_x - \frac{(l_F + l_R) c_R (\dot{V}_y - l_R \ddot{\psi})}{V_x} + \frac{(l_F + l_R) c_R (V_y - l_R \dot{\psi}) \dot{V}_x}{V_x^2} \tag{40}$$

The following form will be derived:

$$\begin{bmatrix} \dot{y}_1 \\ \ddot{y}_2 \end{bmatrix} = \Delta(y_1, y_2, \dot{y}_2) \begin{bmatrix} u_1 \\ u_2 \end{bmatrix} + \Phi(y_1, y_2, \dot{y}_2) \tag{41}$$

Using (35) and (36) for the derivatives of the state variables and the structure of (40), then the following choice can be made:

$$\begin{aligned}
\Delta_{11} =& g_{11} = \frac{1}{mR} \\
\Delta_{12} =& g_{12} = \frac{c_F}{m} \frac{V_y + l_F \dot{\psi}}{y_1} \\
\Delta_{21} =& \frac{c_R (l_F + l_R)(V_y - l_R \dot{\psi}) - l_F m \dot{\psi} y_1^2}{m R y_1^2} \\
\Delta_{22} =& \frac{l_R c_R (l_F + l_R) - l_F m y_1^2}{y_1} \frac{l_F c_F R - l_F I_\omega \dot{\omega}_f}{I_z R} \\
&+ \frac{c_R (l_F + l_R)(V_y - l_R \dot{\psi}) - l_F m \dot{\psi} y_1^2}{y_1^2} \frac{c_F (V_y + l_F \dot{\psi}}{m y_1} \\
&- \frac{c_R (l_F + l_R)}{y_1} \frac{R c_F - I_\omega \dot{\omega}_f}{mR}
\end{aligned} \tag{42}$$

$$\begin{aligned}
\Phi_1 =& f_1(x) + g_{21} \delta^2 = \dot{\psi} V_y - \frac{I_\omega}{mR} (\dot{\omega}_r + \dot{\omega}_f) - \frac{c_F}{m} u_2^2 \\
\Phi_2 =& - l_F m y_1 \left[f_3(x) + g_{13} \gamma(u_1) u_2 \right] \\
&- \frac{(l_F + l_R) c_R}{y_1} \left[f_2(x) + g_{12} \gamma(u_1) u_2 \right] \\
&+ \frac{(l_F + l_R) c_R (V_y - l_R \dot{\psi}) - l_F m \dot{\psi} y_1^2}{y_1^2} \left[f_1(x) + g_{21} u_2^2 \right] \\
&+ \frac{(l_F + l_R) c_R l_R}{y_1} \left[f_3(x) + g_{13} \gamma(u_1) u_2 \right]
\end{aligned} \tag{43}$$

The determinant of the matrix Δ satisfies

$$\begin{aligned}
\det(\Delta) &= \Delta_{11} \Delta_{22} - \Delta_{21} \Delta_{12} \\
&= \frac{(I_\omega \dot{\omega}_f - c_F R) \left[l_F^2 y_1^2 m^2 - c_R (l_F + l_R) l_R l_F m + c_R I_z (l_F + l_R) \right]}{I_z R^2 y_1 m^2} \neq 0
\end{aligned} \tag{44}$$

Then taking into consideration that for typical cars Rc_F/I_ω is around 10^4 and if $I_z > l_F m$ then $c_R(l_R+l_F)(I_z-l_F m)+l_F^2 m^2 y_1^2 \neq 0$, hence neglecting the non-dominant terms $\gamma(u_1)u_2$ and u_2^2 in Φ the control u can be determined from the flatness variables and their derivatives:

$$u = B(y_1, y_2, \dot{y}_1, \dot{y}_2, \ddot{y}_2) = \Delta^{-1}\left(\begin{bmatrix} \dot{y}_1 \\ \ddot{y}_2 \end{bmatrix} - \Phi\right), \quad r_u = 2 \tag{45}$$

Remark: Based on this initial value the control can be further improved by considering the nonlinear terms in Φ and finding the fix point in iterations.

3.4.2 Flatness based control algorithm

For the different flatness variables linear reference systems can be prescribed:

$$\begin{bmatrix} \dot{y}_1 \\ \ddot{y}_2 \end{bmatrix} = \begin{bmatrix} \dot{y}_1^{ref} + k_{1p}e_{y_1} + k_{1I}\int e_{y_1}dt \\ \ddot{y}_2^{ref} + k_{2p}e_{y_2} + k_{2I}\int e_{y_2}dt + k_{2D}\dot{e}_{y_2} \end{bmatrix} \tag{46}$$

where $e_{y_1} = y_1^{ref} - y_1 = V_x^{ref} - V_x$ and $e_{y_2} = e_{y_2}^{ref} - y_2$ and $y_2^{ref} = l_F m V_y^{ref} - Iz\dot{\psi}^{ref}$. The reference signals can be obtained from the high level path design, or in our case from the kinematic control. The angular velocities of the axels can be measured by odometers. All the signals are typically superposed with noises hence reliable filtering and differentiation are needed.

For this purpose Savitzky-Golay filters, fictitious control loops or algebraic estimation can be suggested [12]. From the later two typical methods are presented. Denote $y(t)$ the noisy function to be filtered or differentiated, T is the sampling time. The integration can be performed by the trapezoidal rule.

Filtering using integration:

$$\hat{y}(t) = \frac{2!}{T^2}\int_{t-T}^{t}[-3(t-\tau)+2T]\,y(\tau)d\tau \tag{47}$$

Numerical differentiation using integration:

$$\hat{\dot{y}}(t) = -\frac{3!}{T^3}\int_{t-T}^{t}[2(t-\tau)-T]\,y(\tau)d\tau \tag{48}$$

The steps of the *Flatness Control Algorithm (FCA)*:

1. Reading the signals V_x^{ref}, V_y^{ref}, $\dot{\psi}^{ref}$ from the kinematic control level (or path design) and the signals y_1, y_2, $\dot{y}_2$ from the dynamic system (or its model).
2. Computation of the signals $\hat{y}_1^{ref} = V_x^{ref}$, $\hat{\dot{y}}_1^{ref} = \hat{\dot{V}}_x^{ref}$, $\hat{y}_2^{ref} = l_F m\hat{V}_y^{ref} - I_z\hat{\dot{\psi}}^{ref}$, $\hat{\dot{y}}_2^{ref} = l_F m\hat{\dot{V}}_y^{ref} - I_z\hat{\ddot{\psi}}^{ref}$, $\hat{\ddot{y}}_2^{ref} = l_F m\hat{\ddot{V}}_y^{ref} - I_z\hat{\dddot{\psi}}^{ref}$.

3. Computation of the tracking errors $\hat{e}_{y_1} = \hat{y}_1^{ref} - y_1$, $\hat{e}_{y_2} = \hat{y}_2^{ref} - y_2$, $\hat{\dot{e}}_{y_2} = \hat{\dot{y}}_2^{ref} - \dot{y}_2$.
4. Determine the control signals by

$$u = \begin{bmatrix} T_\omega \\ \delta \end{bmatrix} = \tag{49}$$
$$= \Delta^{-1}(y_1, y_2, \dot{y}_2) \left(\begin{bmatrix} \dot{y}_1^{ref} + k_{1p} e_{y_1} + k_{1I} \int e_{y_1} dt \\ \ddot{y}_2^{ref} + k_{2p} e_{y_2} + k_{2I} \int e_{y_2} dt + k_{2D} \dot{e}_{y_2} \end{bmatrix} - \Phi(y_1, y_2, \dot{y}_2) \right)$$

5. Provide the control signals to the dynamic system.

4 NUMERICAL RESULTS

In the sequel the dynamic control part in the hierarchy will be limited to the nominal control and the DGA methods. Flatness control will be investigated in a separate future paper based on the here developed algorithm.

In order to have comparable results with the approach of Arogeti and Berman [2], we have chosen similar path and vehicle parameters in our experiments, namely $l_R = 1.35$, $l_F = 1.35$, $m_v = 1600$ and $I_{zz} = 2200$ (belonging to COG), all in SI units.

The road-tire relation was described by Pacejka's model:

$$F_{ti} = 2D_M \sin\{C_M \arctan[B_M \alpha_i - E_M \times (B_M \alpha_i - \arctan(B_M \alpha_i)))]\}, \quad i \in \{R, F\}$$

(α_i should be substituted in degree, not in radian). The parameters are $B_M = 0.239$, $C_M = 1.19$, $D_M = 3600\,[N]$ and $E_M = -0.678$. After linear approximation the cornering stiffnesses are $c_R = c_F = 1.1896 \cdot 10^5$ in N/rad.

The reference path is given by

$$y_d = 2\sin(0.25x) + 0.25x + 1, \quad x \in [0, 60]\text{m}$$

which is a straight line with additional slalom.

The velocity limits are $\eta_1 = 8.5$ m/s and $\eta_2 = 9.5$ m/s.

4.1 Checking the available data

For the LMIs the matrices C and D weighting the performance and the magnitude of the control and the disturbance weighting parameter λ were chosen in the referred paper by

$$C = \begin{bmatrix} 1 & 0 & 0 \\ 0 & 1 & 0 \\ 0 & 0 & 3 \\ 0 & 0 & 0 \end{bmatrix}, \quad D = \begin{bmatrix} 0 \\ 0 \\ 0 \\ 1/v(t) \end{bmatrix}$$

where $D(4)$ was corrected to make $\bar{C}$ constant which is necessary to the cited theory.

We have corrected the formula for the disturbance bounds and obtained that the Frobenius norm should be used. With its use the supremum of the Frobenius norm of $B_1(t)B_1^T(t)$ along the path is 1.8174 and its square root is 1.3446, so that its upper bound can be chosen as

$$\bar{B}_1 = 1.3446 \begin{bmatrix} 1 & 0 & 0 \\ 0 & 1 & 0 \\ 0 & 0 & 1 \end{bmatrix}$$

which is in good correspondence ($1.35I_3$) of the referred paper.

Using the above paper's result $1.35I_3$, the solutions of the two LMIs have also been determined:

$$Q = \begin{bmatrix} 12.9587 & -3.4709 & -0.4358 \\ -3.4709 & 2.1682 & -1.1092 \\ -0.4358 & -1.1092 & 1.4821 \end{bmatrix}$$
$$Y = \begin{bmatrix} 1.0548 & -0.9856 & -0.9252 \end{bmatrix}$$
$$K = \begin{bmatrix} -1.9357 & -6.7468 & -6.2429 \end{bmatrix}$$

The state feedback $K = \begin{bmatrix} -1.9 & -6.7 & -6.2 \end{bmatrix}$ is in good correspondence with the paper's solution which will be used later on.

4.2 The nonlinear dynamic model and the DGA control

The kinematic control and the dynamic control are running in different frames, and the dynamic modeling too. The velocity computation between them is as usual. Denote v_K the velocity vector at the origin of the kinematic frame (origin on the rear axle) and v_C the velocity of the origin of the dynamical frame (at the CoG), respectively. Using two dimensional vectors, the transformations between them are as follows:

$$\begin{aligned} v_C &= v_K + \begin{bmatrix} 0 & -1 \\ 1 & 0 \end{bmatrix} l_R \dot{\psi} \\ a_C &= \dot{v}_C + \begin{bmatrix} 0 & -1 \\ 1 & 0 \end{bmatrix} \dot{\psi} v_C \\ v_F &= v_K + \begin{bmatrix} 0 & -1 \\ 1 & 0 \end{bmatrix} L\dot{\psi} = v_C + \begin{bmatrix} 0 & -1 \\ 1 & 0 \end{bmatrix} l_F \dot{\psi} \\ a_K &= \dot{v}_K + \begin{bmatrix} 0 & -1 \\ 1 & 0 \end{bmatrix} \dot{\psi} v_K \end{aligned} \tag{50}$$

From the velocities of the axles the slip angles can be determined and used to find the lateral forces by Pacejka's Magic Formula. For rear driving ($F_{xR} = F_{lR}$, $F_{yR} = F_{lR}$)

and front steering (which is assumed, $F_{xF} = F_{lF} = 0$, $F_{yF} = F_{tF}$) the dynamic motion equations for plane motion are given as

$$m_v a_C = \begin{bmatrix} C_{\delta_w} & -S_{\delta_w} \\ S_{\delta_w} & C_{\delta_w} \end{bmatrix} \begin{bmatrix} 0 \\ F_{yF} \end{bmatrix} + \begin{bmatrix} F_{xR} \\ F_{yR} \end{bmatrix}$$
$$I_{zz}\ddot{\psi} = l_F F_{yF} C_{\delta_w} - l_R F_{yR} \tag{51}$$

The differential equations (51) of the dynamic model and those consisting of (6) for the kinematic model are parallel running. From the differential equations the state equations can easily be formed.

For DGA control the higher order derivatives of the desired path by the time are needed. For this purpose the function `movingslope` is used which is available in MATLAB environment. This method of John D'Errico (woodchips@rochester.rr.com) uses filter to determine the slope of a curve stored as an equally spaced sequence of points. With 3 point window the method is similar to the derivation. It was used three times assuming constant speed 9 m/s along the prescribed path. Notice, that two path design is necessary, one for the K–frame origin and another for the C–frame origin.

The continuous time models and the DGA controller were discretized by Euler method with sampling time $T_S = 0.01$ sec and used in the realization.

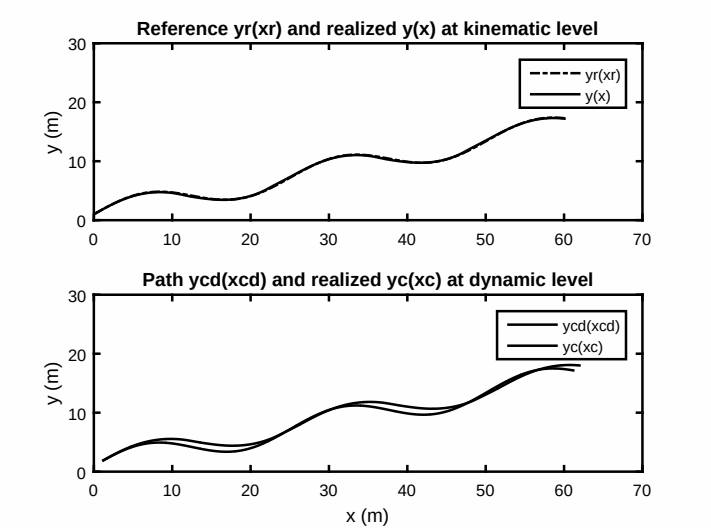

Figure 2
Kinematic and nominal control results

4.3 Simulation results

Simulation experiments were performed with high level modified kinematic control and low level nominal and DGA controls. Kinematic and dynamical controls are

running parallel, the latter supplies the kinematic control with the slipping angles.

The path design is performed in K-frame and the path is transformed to the C-frame using (50). The constant state feedback matrix $K = YQ^{-1}$ is computed offline from the solution of (12). The nominal dynamic control is based on (15). The DGA control was deeply described in the steps of the *DGA Control Algorithm*.

Denote $X_c = (v_B, x_c, y_c, \psi, \dot{\psi}, \delta_W)^T$ the state and $U_c = (F_{lR}, \dot{\delta}_w = w)^T$ the control of the C-frame. Let $X_k = (x, y, \psi, \delta_w)^T$ be the state and $U_k = (v_r, u, w = \dot{\delta}_w)^T$ the control of the K-frame, i.e. the middle point of the of the rear axle. The kinematic control is based on X_k and the slip angles $\alpha_R = \alpha_1$ and $\alpha_F = \alpha_2$ are determined from the dynamic control using Pacejka's magic formula. Non-measurable state variables can be determined in real time by the fusion of a common sensory system and state estimation for all the control methods. Since they are common for all the controllers, hence in the simulation they are emulated by the integration of the dynamics of X_c. Two position vectors can be computed for the CoG, p_{cc} from X_c and another p_{ck} from X_k.

The cycle of the simulation for one sampling instant T_s repeats the following steps:

1. Reading X_c and p_{ck}. Compute $v_R, v_F, \alpha_R, \alpha_F, \beta$ from X_c.
2. Reading X_k and p_{ck}. Compute the path $y_d(x) = f(x)$ and its derivatives $f'(x)$, $f''(x)$, $f'''(x)$.
3. Determine the kinematic error $e = (e_1, e_2, e_3)^T$.
4. Compute the kinematic control, i.e. choose v_r and use the state feedback matrix to compute the kinematic control $u = K * e * v_r$ and $w = \dot{\delta}_w$.
5. Integrate the kinematic state equation by computing the derivatives at the right side of the DE and using Euler method for the new X_k and p_{ck}.
6. Determine the transversal forces $F_R = F_1$ and $F_F = F_2$ using Pacejka's formula.
7. Perform numerical differentiations for the necessary variables and compute the new internal states needed to them.
8. Compute the control outputs F_{lR} and $w = \dot{\delta}_w$ for nominal control, and S_h, u_1, $u_2 = F_{lR}$ and $w = \dot{\delta}_w$ for the DGA algorithm, respectively.
9. Model the saturation of the control forces between $\pm$8000N.
10. Integrate the dynamic state equation by computing the derivatives at the right side of the DE and using Euler method for computing the new X_c and p_{cc}.
11. Storing the new states X_c, p_{cc} and the new control signals U_c for dynamic control, and the new states X_k, p_{ck} and the new control signals U_k for kinematic control.

Fig. 2 and Fig. 4 show that the kinematic level works well in the presence of acceptable rear and front slip angles, see also Fig. 3 and Fig. 5. The steering angles are in acceptable domains. From the lower part of Fig. 2 can be seen the main result

that if the steering angle is saved in the dynamic control (e.g. modeling an industrial controller with quick transients) than lateral errors of order 1m can be observed which may be critical in case of UGVs if no visual information for correction is available. This can be seen deeper in Fig. 6 for both dynamical control forms. For DGA it can also be seen that, although the nonlinear input–output linearization (DGA) can well stabilize the system, it cannot essentially decrease the lateral error.

5 CONCLUSION

In this paper the problem of the hierarchical control of UGVs was considered. High level kinematic control in the presence of sliding effects was analyzed using the modified kinematic control method of Arogeti and Berman. The non-published derivations of some important details were checked. In order to improve the precision of the path tracking low level nonlinear dynamic control methods were suggested. Novelties of our paper are:

i) Development of three low level techniques: nominal, DGA and flatness based dynamic control methods to supply the high level modified kinematic control with realistic front and rear sliding angles.

ii) The high level modified kinematic control method can well tolerate the sliding angles in the realistic domain of less than 15 degree and the path errors remain small at kinematic level.

iii) Using the nominal control it was experimentally proven the fact that if the steering angle of the kinematic control is used as the reference signal for the low level (e.g. industrial) steering control then this approach may cause problems for UGVs because the lateral error is in the order of 1m. This may be critical in the lack of visual information since no driver is present to make corrections.

iv) Simple methods, like nonlinear input–output linearization in the form of the DGA dynamic control with own reference signals (i.e. the path), can stabilize the vehicle but cannot considerably decrease the lateral error.

Further researches are necessary to develop new dynamic control methods that are able to decrease the path errors and are simple enough for real-time implementation. The flatness based control is one of the methods in this direction. A future paper will consider this investigation based on the here presented approach.

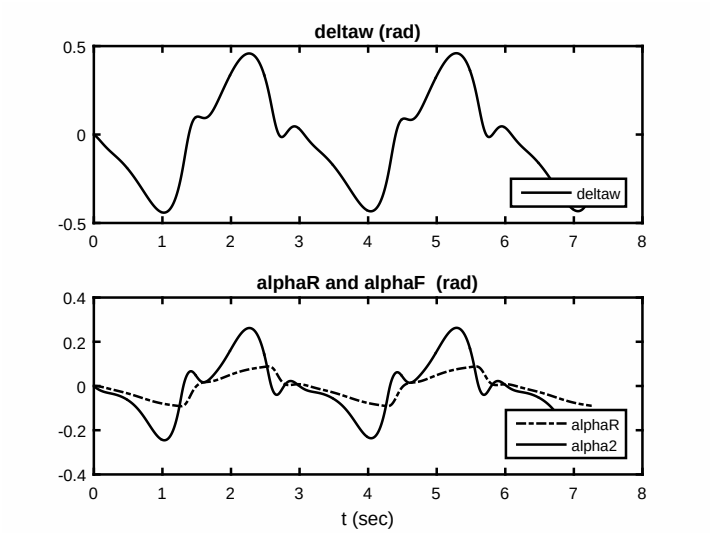

Figure 3
Steering and slipping angles with nominal control

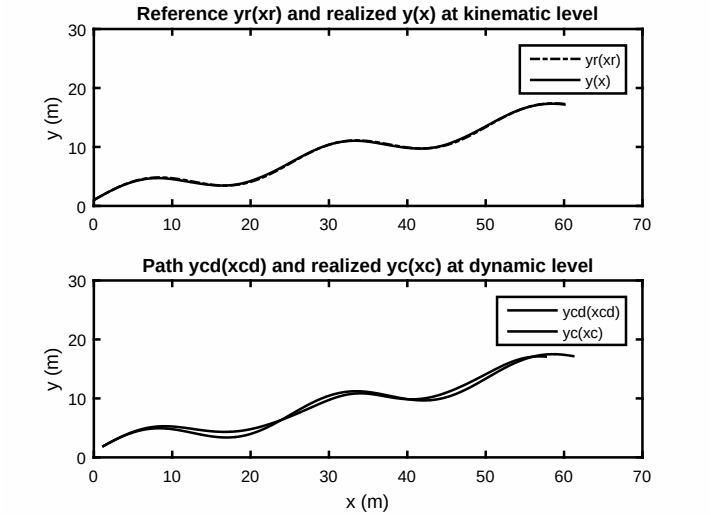

Figure 4
Kinematic and DGA control results

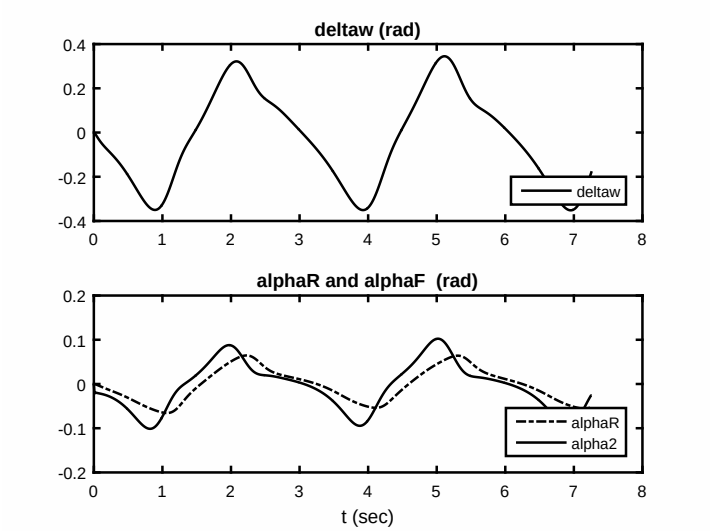

Figure 5
Steering and slipping angles with DGA control

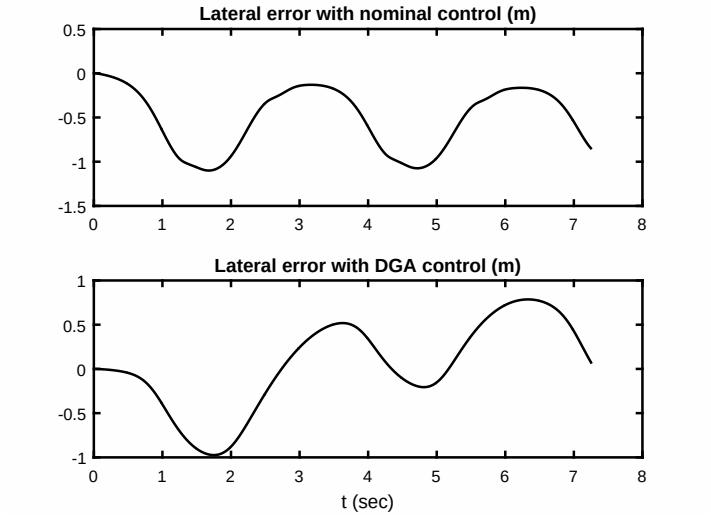

Figure 6
Lateral errors with nominal and DGA control

Acknowledgements

The research of B. Lantos was supported by the MTA-BME Control Engineering Research Group.

References

[1] A. D. Luca, G. Oriolo, and C. Samson, *Feedback control of a nonholonomic car-like robot*. J.P. Laumond, Ed. ser. Lecture Notes in Control and Information Sciences, Springer Verlag, New York, 1998.

[2] A. Arogeti and N. Berman, "Path following of autonomous vehicles in the presence of sliding effects." *IEEE Transaction on Vehicular Technology*, vol. 61, no. 4, pp. 1481–1492, 2012.

[3] C. Scherer and S. Weiland, *Lecture Notes DISC Course on Linear Matrix Inequalities in Control, ver. 2.0, pp. 50–57*, 1999.

[4] Z. Bodó and B. Lantos, "Error caused by kinematic control in dynamic behavior of unmanned ground vehicles," in *IEEE Symposium on Applied Computational Intelligence and Informatics SACI2018*, Timisoara, Romania, May 2018, pp. 1–6.

[5] R. Rajamani, *Vehicle dynamics and control*. Springer, New York, 2006.

[6] L. Talvala, K. Kritayakirana, and J. Gerdes, "Pushing the limits: From lane-keeping to autonomous racing." *Annu. Rev. Control*, vol. 35, no. 1, pp. 137–148, 2011.

[7] G. Max and B. Lantos, "Time optimal control of four-in–wheel-motors driven electric cars." *Periodica Polytechnica Electrical Engineering and Computer Science*, vol. 58, no. 4, pp. 149–159, 2014.

[8] H. Pacejka, *Tire and vehicle dynamics*. SAE International, 2005.

[9] B. Lantos and L. Marton, *Nonlinear control of vehicles and robots*. Springer, London, 2011.

[10] M. Fliess, J. Levine, P. Martin, and P. Rouchon, "Lie–Bäcklund approach to equivalence and flatness of nonlinear systems," *IEEE Transaction on Automatic Control*, vol. 44, no. 5, pp. 922–937, May 1999.

[11] L. Menhour, B. d'Andrea Novel, M. Fliess, and H. Mounier, "Coupled nonlinear vehicle control: Flatness-based setting with algebraic estimation techniques." *Control Engineering Practice*, vol. 22, 2014.

[12] E. Diekema and T. Koornwinder, "Differentiation by integration using orthogonal polynomials, a survey," *Journal of Approximation Theory*, vol. 164, 2012.